



RESEARCH LETTER

10.1002/2016GL068513

Key Points:

- Aquatic plant leaf wax hydrogen isotopes at this study site reflect precipitation seasonality
- Winter snowfall on western Greenland was highest 6 to 4 ka, coincident with sea ice minima
- Increased winter snowfall may explain minimal Holocene Greenland Ice Sheet retreat

Supporting Information:

- Supporting Information S1
- Table S1
- Table S2
- Table S3
- Table S4

Correspondence to:

E. K. Thomas,
ekthomas@buffalo.edu

Citation:

Thomas, E. K., J. P. Briner, J. J. Ryan-Henry, and Y. Huang (2016), A major increase in winter snowfall during the middle Holocene on western Greenland caused by reduced sea ice in Baffin Bay and the Labrador Sea, *Geophys. Res. Lett.*, 43, doi:10.1002/2016GL068513.

Received 3 MAR 2016

Accepted 21 APR 2016

Accepted article online 25 APR 2016

A major increase in winter snowfall during the middle Holocene on western Greenland caused by reduced sea ice in Baffin Bay and the Labrador Sea

Elizabeth K. Thomas^{1,2}, Jason P. Briner², John J. Ryan-Henry^{3,4,5}, and Yongsong Huang^{3,6}

¹Department of Geosciences, University of Massachusetts Amherst, Amherst, Massachusetts, USA, ²Department of Geology, University at Buffalo, Buffalo, New York, USA, ³Department of Earth, Environment and Planetary Sciences, Brown University, Providence, Rhode Island, USA, ⁴Department of Marine Affairs, University of Rhode Island, Kingston, Rhode Island, USA, ⁵Roger Williams University School of Law, Bristol, Rhode Island, USA, ⁶Institute of Earth Environment, Chinese Academy of Sciences, Xi'an, China

Abstract Precipitation is predicted to increase in the Arctic as temperature increases and sea ice retreats. Yet the mechanisms controlling precipitation in the Arctic are poorly understood and quantified only by the short, sparse instrumental record. We use hydrogen isotope ratios ($\delta^2\text{H}$) of lipid biomarkers in lake sediments from western Greenland to reconstruct precipitation seasonality and summer temperature during the past 8 kyr. Aquatic biomarker $\delta^2\text{H}$ was 100‰ more negative from 6 to 4 ka than during the early and late Holocene, which we interpret to reflect increased winter snowfall. The middle Holocene also had high summer air temperature, decreased early winter sea ice in Baffin Bay and the Labrador Sea, and a strong, warm West Greenland Current. These results corroborate model predictions of winter snowfall increases caused by sea ice retreat and furthermore suggest that warm currents advecting more heat into the polar seas may enhance Arctic evaporation and snowfall.

1. Introduction

Arctic precipitation is predicted to increase as climate warms, due to increasing meridional vapor transport and to increasing local evaporation as sea ice retreats [Bintanja and Selten, 2014; Kopec *et al.*, 2016]. Increasing precipitation will be particularly influential over the Greenland Ice Sheet (GrIS). Greenland's proximity to abundant North Atlantic moisture sources is likely one of the main reasons that the GrIS persisted during interglacial periods, when other Northern Hemisphere ice sheets succumbed to rising temperature. Greenland's ice mass loss, which is important for sea level rise, is predicted to increase in the coming century, but the rate of ice mass loss is poorly constrained [Church *et al.*, 2013]. Paired climate and ice sheet records from previous warm periods can elucidate the factors influencing GrIS mass balance on time scales longer than the observational record [Briner *et al.*, 2016]. During the middle Holocene, temperature on Greenland was $\sim 2^\circ\text{C}$ higher than present [Cuffey and Clow, 1997; Axford *et al.*, 2013]. Yet glacial geologic reconstructions and models indicate that after an early Holocene retreat, the GrIS remained relatively stable from 7 ka to present [Lecavalier *et al.*, 2014; Young and Briner, 2015]. This evidence suggests that some mechanisms, perhaps increasing accumulation, at least partially offset ice mass losses caused by rising temperature.

The seasonality of increasing precipitation in a warming climate is also particularly important for the GrIS. Increased winter accumulation can partially offset mass losses due to rising summer temperature. Increased summer rainfall, however, can enhance ablation via latent heat release when rain refreezes, and transient increases in late-summer ablation can accelerate ice mass loss [Doyle *et al.*, 2015]. Arctic precipitation is difficult to monitor, but existing observations and reanalysis data suggest that reduced sea ice is correlated to increased precipitation [Sodemann *et al.*, 2008; Kopec *et al.*, 2016]. Models predict that 21st century precipitation increases will be greatest in fall and winter, caused by a loss of sea ice during early winter [Bintanja and Selten, 2014]. Evaporation is greatest in the Arctic during early winter and over open water, so a loss of early winter sea ice can cause large increases in evaporation and concomitant increases in early winter snowfall [Bintanja and Selten, 2014].

Hydroclimate and temperature reconstructions during previous warm periods provide climatic context for GrIS changes. Current continuous reconstructions of Holocene hydroclimate are limited to ice cores, from which it is difficult to reconstruct precipitation seasonality [Cuffey and Clow, 1997; Rasmussen *et al.*, 2013]. We use hydrogen isotope ratios ($\delta^2\text{H}$) of lipid biomarkers to reconstruct Holocene precipitation seasonality and temperature

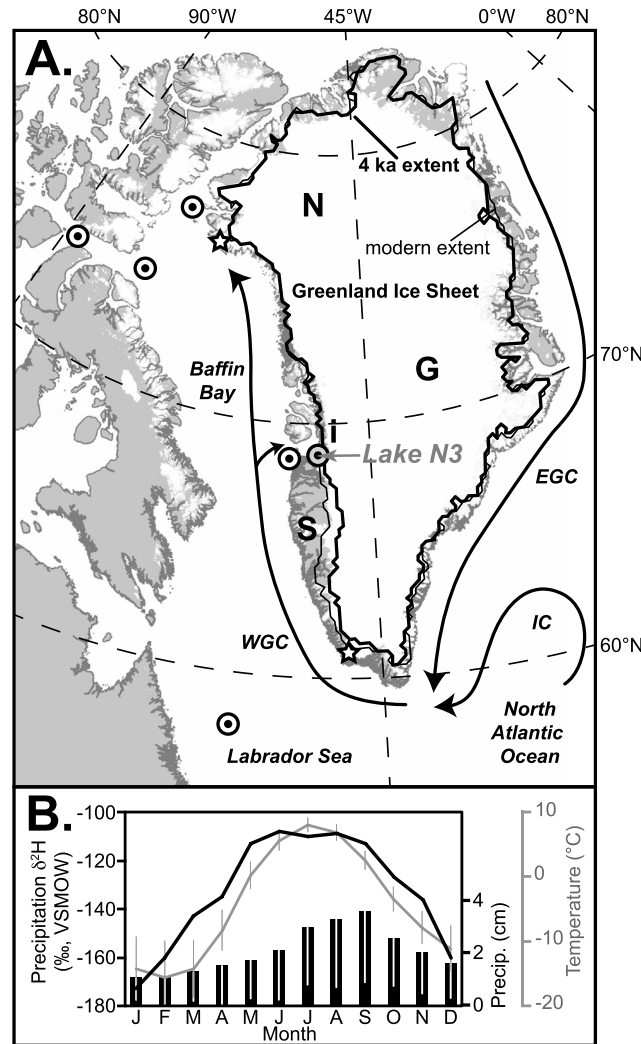


Figure 1. (a) Map of Greenland showing location of Lake N3 (black and gray bulls eye), modeled extents of the GrIS in middle Holocene (bold outline) and modern (fine outline) [Lecavalier et al., 2014], regional ocean currents (WGC = West Greenland Current, IC = Irminger Current, and EGC = East Greenland Current), GNIP stations (stars: Thule (N Greenland); Kangilinnuit (S Greenland)) [IAEA/WMO, 2011], paleoceanographic reconstructions (black and white bulls eyes) [Ledu et al., 2010; de Vernal et al., 2013; Perner et al., 2013; Ouellet-Bernier et al., 2014], and sites mentioned in text (S = Sukkertoppen Ice Cap, i = Ilulissat and North Lake, G = GISP2, and N = NEEM). (b) Monthly temperature, precipitation, and calculated $\delta^2\text{H}_{\text{precip}}$ in Disko Bugt [Bowen et al., 2005; NCDC NOAA, 2012; Bowen, 2016]. Temperature and precipitation calculated for years with complete data, A.D. 1873 to 2013. 1 sigma standard deviations of long-term mean observations shown for temperature (vertical gray lines, $n = 113$) and precipitation (white lines inside of black bars, $n = 117$).

corresponding to large climatic gradients (Figure S3 in the supporting information). Kangilinnuit (southern Greenland) has a maritime climate, with constant $\delta^2\text{H}_{\text{precip}}$ values year round, indicative of a strong influence of local moisture sources [IAEA/WMO, 2011; NCDC NOAA, 2012]. Thule (northern Greenland) has a high-Arctic continental climate, with large-amplitude seasonal changes in temperature and $\delta^2\text{H}_{\text{precip}}$ [IAEA/WMO, 2011; NCDC NOAA, 2012]. Seasonal temperature and $\delta^2\text{H}_{\text{precip}}$ in the Disko Bugt region have similar patterns as at Thule but with muted amplitudes [Bowen et al., 2005; NCDC NOAA, 2012; Bowen, 2016]. The northward decrease in annual average $\delta^2\text{H}_{\text{precip}}$ (-94‰ in southern Greenland, -132‰ in Disko Bugt, and -183‰ in northern

on western Greenland near the GrIS margin, thus better constraining Arctic precipitation responses to changing climate.

2. Methods and Approach

Lake N3 (informal name, 68.636°N , 50.980°W , 59 m above sea level) is a small lake (0.09 km^2 , maximum depth = 16 m) on the Nuuk Peninsula, southeastern Disko Bugt, western Greenland (Figure 1 and Figure S1 in the supporting information). Lake N3 is through-flowing during the ice-free season (May to September) and since deglaciation circa 8 ka has not received melt water from the Greenland Ice Sheet [Young et al., 2013]. Vegetation in the Lake N3 catchment today is dwarf shrub heath, dominated by *Salix* sp. and *Betula* sp. [Bennike, 2000]. Our paleoclimate records are generated from a surface core (10N3-SC) and along core (10N3-2A) collected from deep basins in Lake N3 in August 2010 (Figure S1 in the supporting information). An age-depth model for 10N3-SC was developed by applying a constant rate of supply model to the unsupported ^{210}Pb inventory (Figure S2 and Table S1 in the supporting information). An age-depth model for 10N3-2A was determined using a smooth spline (smoothing level = 0.3) interpolation between eight ^{14}C -dated *Warnstorfia* sp. (aquatic plant) macrofossils (Figure S2 and Table S2 in the supporting information). Bulk and compound-specific geochemical analyses followed previously published methods [Thomas et al., 2011, 2012] (the supporting information).

Today, there are large precipitation hydrogen isotope ($\delta^2\text{H}_{\text{precip}}$) gradients on western Greenland, corre-

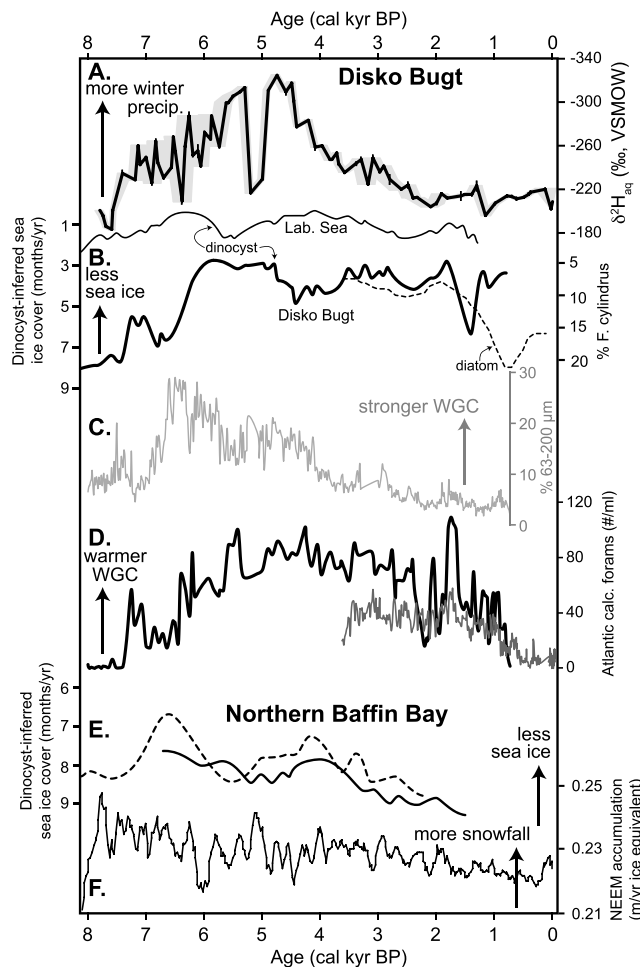


Figure 2. (a) Lake N3 $\delta^2\text{H}_{\text{aq}}$ (y axis inverted, gray shading = 95% age model uncertainty, vertical black lines = analytical uncertainty). (b) Months with greater than 50% sea ice cover inferred from dinocysts in the Labrador Sea (fine line) and Disko Bugt (bold line), and abundance of sea ice-associated diatom *Fragilariopsis cylindrus* Disko Bugt (dashed line) [de Vernal et al., 2013; Krawczyk et al., 2013; Ouellet-Bernier et al., 2014]. Data smoothing is from original publications. (c) Percent fine sand in Disko Bugt sediments, indicative of West Greenland Current strength [Perner et al., 2013]. (d) Concentration of Atlantic calcareous benthic foraminifera from two cores, indicative of warm West Greenland Current [Perner et al., 2013]. (e) Months with sea ice cover > 50% inferred from dinocysts in northern Baffin Bay [Ledu et al., 2010; de Vernal et al., 2013]. Data smoothing is from original publications. (f) Accumulation at NEEM ice core site [Rasmussen et al., 2013].

We reconstruct precipitation seasonality using $\delta^2\text{H}$ of C_{24} *n*-alkanoic acids, produced mainly by aquatic macrophytes and by bryophytes ($\delta^2\text{H}_{\text{aq}}$, Figure 2 and Figure S4 in the supporting information) [Nichols et al., 2009]. Aquatic plants use lake water as the source for leaf wax production, so $\delta^2\text{H}_{\text{aq}}$ changes as a function of lake water $\delta^2\text{H}$. We calculate Lake N3 water residence time to be 13 ± 3 months (Table S3 in the supporting information). The lake is not subject to strong evaporative enrichment because it has continuous through-flow during the short ice-free season [Jonsson et al., 2009]. Lake water $\delta^2\text{H}$ therefore reflects annual mean $\delta^2\text{H}_{\text{precip}}$. This relationship is corroborated by modern aquatic plant *n*-alkyl lipid $\delta^2\text{H}$ measurements at Lake N3 (Table S4 in the supporting information). Due to the large seasonal range of $\delta^2\text{H}_{\text{precip}}$ at Lake N3 (Figure 1), an increase in winter snowfall relative to summer precipitation would result in a ^2H -depletion of amount-weighted annual mean $\delta^2\text{H}_{\text{precip}}$, and vice versa. Thus, we infer changes in precipitation seasonality from $\delta^2\text{H}_{\text{aq}}$ (Figure 2).

Greenland) but increase in seasonal $\delta^2\text{H}_{\text{precip}}$ amplitudes along western Greenland is likely a result of a northward increase in distillation during vapor transport [Jouzel et al., 1997]. Distillation and temperature are negatively correlated, and as a result, the modern temperature- $\delta^2\text{H}_{\text{precip}}$ relationship increases northward along western Greenland, from $-0.1\text{‰}\text{C}^{-1}$ at Kangilinnuit to $3.4\text{‰}\text{C}^{-1}$ at Thule [IAEA/WMO, 2011] (Figure S3 in the supporting information). Temperature- $\delta^2\text{H}_{\text{precip}}$ relationships likely changed through time, as an increase in sea ice cover would increase transport distance and cause more distillation during transport [Jouzel et al., 1997; Faber et al., 2015]. Thus, even if temperature is the main mechanism influencing past $\delta^2\text{H}_{\text{precip}}$, records of precipitation isotopes in this region should be used to infer only qualitative changes in temperature, unless independent constraints can be placed on the temperature- $\delta^2\text{H}_{\text{precip}}$ paleo-relationship.

We generate Holocene records of precipitation seasonality and summer temperature changes using leaf wax $\delta^2\text{H}$. $\delta^2\text{H}$ of leaf waxes from surface sediments in temperate lakes and in Arctic lakes that experience minimal evaporative enrichment is correlated with precipitation and lake water $\delta^2\text{H}$, offset by a biosynthetic fractionation that is largely constant on the catchment scale for specific compounds [Sachse et al., 2012; Thomas et al., 2012; Shanahan et al., 2013].

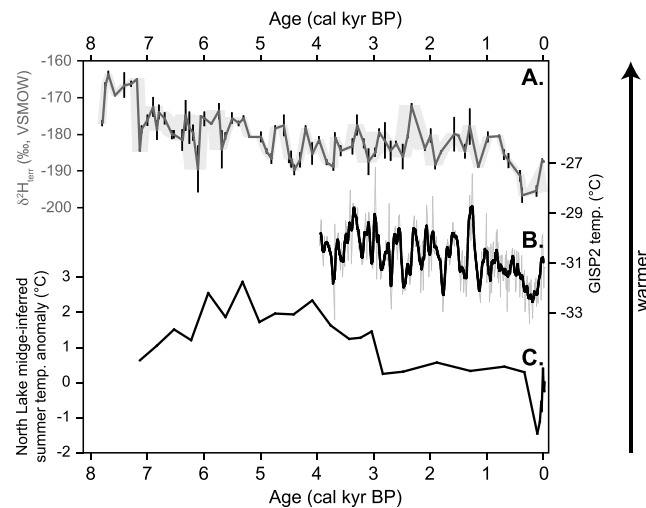


Figure 3. (a) Lake N3 $\delta^2\text{H}_{\text{terr}}$ (gray shading = 95% age model uncertainty and vertical black lines = analytical uncertainty). (b) Mean annual snow temperature at GISP2 [Kobashi *et al.*, 2011]. Bold black line is a 51 year running mean, fine gray line is raw annual data. (c) Midge-inferred average summer temperature anomaly at North Lake [Axford *et al.*, 2013].

We reconstruct qualitative summer temperature using $\delta^2\text{H}$ of C_{28} *n*-alkanoic acids, produced by terrestrial plants ($\delta^2\text{H}_{\text{terr}}$, Figure 3 and Figure S4 in the supporting information). Terrestrial plants likely synthesize leaf waxes at leaf flush, which occurs in June in modern western Greenland, and throughout the subsequent growing season [ORNL DAAC, 2008; Gao *et al.*, 2012; Tipple *et al.*, 2013]. This relationship is corroborated by modern terrestrial plant *n*-alkyl lipid $\delta^2\text{H}$ measurements at Lake N3 (Table S4 in the supporting information). The vapor sources for precipitation on western Greenland, Baffin Bay, and the Labrador and Irminger Seas [Ohmura and Reeh, 1991; Sodemann *et al.*, 2008] were ice free during summer throughout the Holocene [de Vernal *et al.*, 2013;

Ouellet-Bernier *et al.*, 2014], so source areas of summer precipitation for western Greenland likely did not change, and temperature was the main mechanism influencing Holocene summer $\delta^2\text{H}_{\text{precip}}$. Thus, we interpret $\delta^2\text{H}_{\text{terr}}$ to indicate qualitative centennial-scale changes in Holocene summer temperature on western Greenland.

Terrestrial plant source water in the Lake N3 catchment (soil water) is primarily derived from summer rainfall, but may contain some winter snowmelt, as Arctic soil water residence time is approximately 1 month [Cooper *et al.*, 1991]. Thus, the orbital-scale changes in precipitation seasonality inferred from $\delta^2\text{H}_{\text{aq}}$ likely influence $\delta^2\text{H}_{\text{terr}}$ (supporting information). We can use $\delta^2\text{H}_{\text{aq}}$ to remove the effect of precipitation seasonality from $\delta^2\text{H}_{\text{terr}}$, but this method involves multiple assumptions (Figure S5 in the supporting information). We therefore interpret only the centennial-scale changes in Lake N3 $\delta^2\text{H}_{\text{terr}}$ and use independent temperature reconstructions to infer orbital-scale terrestrial summer temperature changes on western Greenland [Axford *et al.*, 2013].

3. Holocene Summer Temperature on Western Greenland

Our interpretation of Lake N3 $\delta^2\text{H}_{\text{terr}}$ as summer temperature is supported in several ways (Figure 3). First, $\delta^2\text{H}_{\text{terr}}$ exhibits similar centennial-scale patterns during the past ~ 300 years as midge-inferred summer temperature anomalies at North Lake, western Greenland (Figure 3c) [Axford *et al.*, 2013]. Coldest conditions in both records correspond with the Little Ice Age and end with warming in recent decades, a pattern also documented in Disko Bugt [Perner *et al.*, 2013]. Second, the centennial-scale variability in Lake N3 $\delta^2\text{H}_{\text{terr}}$ is remarkably similar to the 4 kyr-long record of annual average surface temperature at Greenland Ice Sheet Project 2 (GISP2), Greenland ($r^2 = 0.43$) [Kobashi *et al.*, 2011] (Figure 3b and Figure S5 in the supporting information), suggesting similar controls on late Holocene centennial-scale temperature at these sites, despite seasonal and elevation differences.

The modern summer $\delta^2\text{H}_{\text{precip}}$ gradient on western Greenland provides an analog for Holocene summer temperature changes recorded by Lake N3 $\delta^2\text{H}_{\text{terr}}$. Modern summer $\delta^2\text{H}_{\text{precip}}$ at Kangilinnuit (southern Greenland, subarctic climate) is $\sim 60\text{‰}$ higher than at Thule (northern Greenland, high Arctic climate) and 20‰ higher than at Lake N3 (Figure 1 and Figure S3 in the supporting information). Analogously, from 8 to 5 ka, Lake N3 $\delta^2\text{H}_{\text{terr}}$ was 10 to 20‰ higher than during recent decades, indicative of a warm, maritime climate similar to modern summers at Kangilinnuit (Figure 3a). During the middle to late Holocene, the West Greenland Current weakened and the sea ice front migrated south, causing cooling on western Greenland (Figure 2) [Perner *et al.*, 2013; Ouellet-Bernier *et al.*, 2014]. This cooling is reflected in $\delta^2\text{H}_{\text{terr}}$, which had values similar to present from 4.5 to 0.3 ka, indicative of an increasingly cold, Arctic climate. The coldest conditions inferred from Lake N3 $\delta^2\text{H}_{\text{terr}}$ occurred during the Little Ice Age, circa 1600 to 1900 A.D. in this record (Figure 3).

4. Holocene Precipitation Seasonality on Western Greenland

Lake N3 $\delta^2\text{H}_{\text{aq}}$ has a $>100\%$ range during the past 8 kyr, larger than the range of modern seasonal $\delta^2\text{H}_{\text{precip}}$ in Disko Bugt (Figures 1 and 2a). We interpret these large changes in $\delta^2\text{H}_{\text{aq}}$ to indicate changes in precipitation seasonality, with Arctic moisture sources contributing to the exceptionally low $\delta^2\text{H}$ values. The magnitude and direction of $\delta^2\text{H}_{\text{aq}}$ changes cannot be explained by changes in terrestrial plant contributions of C_{24} n -alkanoic acids, by Holocene temperature change, or by lake water residence time (Figures S6 and S7 in the supporting information).

Lake N3 $\delta^2\text{H}_{\text{aq}}$ decreased steadily from -190 to -300% from 7.5 to 6 ka, in step with declining sea ice in Disko Bugt (Figures 2a and 2b) [Ouellet-Bernier et al., 2014]. Lake N3 $\delta^2\text{H}_{\text{aq}}$ remained low during the middle Holocene, synchronous with minimum regional sea ice. The Labrador Sea, an important moisture source region for western Greenland [Sodemann et al., 2008], had minimum sea ice cover from 6.5 to 3.5 ka (Figure 2b) [de Vernal et al., 2013]. Furthermore, sea ice reached a minimum in northern Baffin Bay and the Canadian Arctic from 6 to 3 ka [Ledu et al., 2010; de Vernal et al., 2013], creating a source for moisture that was ^2H -depleted compared to modern winter precipitation around Lake N3. Although Baffin Bay still had seasonal sea ice during the middle Holocene, sea ice would have formed later in the year [Markus et al., 2009]. A loss of sea ice during early winter, when evaporation is greatest, can cause large increases in early winter snowfall [Bintanja and Selten, 2014]. Finally, the West Greenland Current was both strong and warm 6 to 4 ka, likely due to an increased contribution of the warm Irminger Current to the West Greenland Current, resulting in regional warmth and providing energy to evaporate more moisture (Figures 2c and 2d) [Perner et al., 2013]. Winter insolation was low during the middle Holocene [Laskar et al., 2004], so there was likely a large contrast between winter air temperature and winter ocean surface temperature. This temperature contrast would cause high evaporation. Thus, we interpret the significant middle Holocene depletion of Lake N3 $\delta^2\text{H}_{\text{aq}}$ as an increase in winter precipitation, caused by the near total loss of sea ice cover in the Labrador Sea, and the loss of early winter sea ice and increased oceanic heat advection in Baffin Bay. This relationship has been identified elsewhere on Greenland. The millennial-scale trend of Holocene accumulation at the North Greenland Eemian Ice Drilling Site (NEEM) in northwestern Greenland tracks, and may have been caused by, changes in sea ice cover in northern Baffin Bay (Figures 2e and 2f), supporting our inference that Holocene precipitation trends can be closely linked to sea ice cover [Ledu et al., 2010; de Vernal et al., 2013; Rasmussen et al., 2013].

A brief ^2H -enrichment of Lake N3 $\delta^2\text{H}_{\text{aq}}$ from 5.2 to 5.0 ka coincides with an abrupt decline in organic matter in Lake N3 sediments, indicative of reduced primary productivity (Figure S7 in the supporting information). The ^2H -enrichment may have been caused by brief increases in sea ice cover in the Labrador Sea and Disko Bugt (Figure 2b) [de Vernal et al., 2013; Ouellet-Bernier et al., 2014]. There is also evidence for a decrease in West Greenland Current strength and temperature ~ 5 ka, which would decrease heat advection to the region (Figures 2c and 2d) [Perner et al., 2013]. Both of these mechanisms would have caused regional cooling and a decline in primary productivity, as well as reduced evaporation, causing less snowfall and an increase in $\delta^2\text{H}_{\text{aq}}$.

After 4 ka, $\delta^2\text{H}_{\text{aq}}$ increased rapidly to -240% at 3.5 ka and then gradually to -210% at 2 ka, after which $\delta^2\text{H}_{\text{aq}}$ remained stable (Figure 2a). We interpret this increase in $\delta^2\text{H}_{\text{aq}}$ as a decrease in winter precipitation, which coincides with rapid cooling recorded by lakes near Ilulissat [Axford et al., 2013]. Although the West Greenland Current remained warm until ~ 2 ka, the current weakened at 4 ka, reducing heat advection to Baffin Bay (Figures 2c and 2d) [Perner et al., 2013]. Additionally, gradually increasing winter insolation would have resulted in a smaller winter ocean-air thermal contrast, reducing evaporation. Evaporation would have been further reduced by increasing sea ice cover in northern Baffin Bay (Figure 2e) [Ledu et al., 2010; de Vernal et al., 2013]. The increase in northern Baffin Bay sea ice would have cut off the supply of ^2H -depleted Arctic moisture to Disko Bugt [Rasmussen et al., 2013]. Sea ice in Disko Bugt did not increase until ~ 1 ka, after Lake N3 $\delta^2\text{H}_{\text{aq}}$ had reached stable late Holocene values (Figure 2b) [Krawczyk et al., 2013]. The steady decrease in winter snowfall from 4.5 to 2 ka instead likely was caused by increased early winter sea ice cover in northern Baffin Bay and the Labrador Sea, and cooler regional surface ocean temperatures, phenomena that are likely linked to regional late Holocene cooling (Figure 3) [Kobashi et al., 2011; Axford et al., 2013; de Vernal et al., 2013].

5. The GrIS Response to Increasing Middle Holocene Winter Precipitation

The middle Holocene increase in winter snowfall recorded by Lake N3 $\delta^2\text{H}_{\text{aq}}$ may account for the spatial patterns of Holocene GrIS change. Despite warmer summers, the western GrIS retreated very little during the middle

Holocene (Figure 1) [Lecavalier *et al.*, 2014; Young and Briner, 2015]. We hypothesize that increased winter precipitation on the western GrIS during the middle Holocene (Figure 2a) may have offset a portion of ablation at the GrIS margin caused by warmer summers (Figure 3). A possible exception to this minimal middle Holocene retreat is the portion of the Greenland Ice Sheet inland of the Sukkertoppen Ice Cap, south of Lake N3, which is the only portion of the Greenland Ice Sheet modeled to have significant (~ 50 km) retreat (Figure 1) [Lecavalier *et al.*, 2014]. This portion of the ice sheet is in an orographic shadow [Ohmura and Reeh, 1991; Bales *et al.*, 2009] and therefore may not have experienced increased winter precipitation during the middle Holocene, perhaps making this portion of the ice sheet more sensitive to rising summer temperature. Our results at Lake N3 suggest that changes in the amount of accumulation on the western GrIS are likely controlled by sea ice cover in the Labrador Sea and Baffin Bay, and by the strength and temperature of the West Greenland Current.

6. Conclusions

Lipid biomarker $\delta^2\text{H}$ data demonstrate that although western Greenland was warmer during the middle Holocene, this region experienced increased snowfall. The middle Holocene increase in snowfall was likely caused by a combination of decreased early winter sea ice cover and increased heat advection to Baffin Bay. Relatively rapid changes in winter snowfall ~ 5 and 4.5 ka indicate that Arctic hydroclimate is sensitive to changes in ocean surface conditions, including sea ice and ocean heat content. The response of the western GrIS to higher summer temperatures may have been muted due to increased accumulation in the middle Holocene. Our results suggest that in the future, as Arctic seas warm and sea ice retreats, increased winter precipitation may enhance accumulation on parts of the GrIS and partly offset summer ablation, particularly in areas close to modern winter sea ice fronts.

Acknowledgments

This research was supported by a Geological Society of America (GSA) student research grant, a GSA Limnogeology Division Kerry Kelts Research Award, a GSA Quaternary Geology and Geomorphology Division Marie Morisawa Research Award, and an NSF Graduate Research Fellowship to E. K.T., NSF award 909334 to J.P.B., and NSF award 0520718 to Y.H. E.K.T. is currently an NSF EAR Postdoctoral Fellow, NSF award 1349595. We thank Rafael Tarozo and Shanna Losee for lab support. Lake N3 chronological and geochemical data are freely available at the NOAA/World Data Center for Paleoclimatology (<https://ncdc.noaa.gov/paleo/study>).

References

- Axford, Y., S. Losee, J. P. Briner, D. R. Francis, P. G. Langdon, and I. R. Walker (2013), Holocene temperature history at the western Greenland ice sheet margin reconstructed from lake sediments, *Quat. Sci. Rev.*, *59*, 87–100, doi:10.1016/j.quascirev.2012.10.024.
- Bales, R. C., Q. Guo, D. Shen, J. R. McConnell, G. Du, J. F. Burkhart, V. B. Spikes, E. Hanna, and J. Cappelén (2009), Annual accumulation for Greenland updated using ice core data developed during 2000–2006 and analysis of daily coastal meteorological data, *J. Geophys. Res.*, *114*, D06116, doi:10.1029/2008JD011208.
- Bennike, O. (2000), Palaeoecological studies of Holocene lake sediments from west Greenland, *Palaeogeogr. Palaeoclimatol. Palaeoecol.*, *155*(3–4), 285–304, doi:10.1016/S0031-0182(99)00121-2.
- Bintanja, R., and F. M. Selten (2014), Future increases in Arctic precipitation linked to local evaporation and sea-ice retreat, *Nat. Adv. Online Publ.*, doi:10.1038/nature13259.
- Bowen, G. J. (2016), OIPC: The online isotopes in precipitation calculator, version 2.2. [Available at www.waterisotopes.org.]
- Bowen, G. J., L. I. Wassenaar, and K. A. Hobson (2005), Global application of stable hydrogen and oxygen isotopes to wildlife forensics, *Oecologia*, *143*(3), 337–348.
- Briner, J. P., *et al.* (2016), Holocene climate change in Arctic Canada and Greenland, *Quat. Sci. Rev.*, doi:10.1016/j.quascirev.2016.02.010.
- Church, J. A., *et al.* (2013), Sea level change, in *Climate Change 2013: The Physical Science Basis. Contribution of Working Group I to the Fifth Assessment Report of the Intergovernmental Panel on Climate Change*, edited by T. F. Stocker *et al.*, Cambridge Univ. Press, Cambridge, U. K., and New York.
- Cooper, L. W., C. R. Olsen, D. K. Solomon, I. L. Larsen, R. B. Cook, and J. M. Grebmeier (1991), Stable isotopes of oxygen and natural and fallout radionuclides used for tracing runoff during snowmelt in an Arctic watershed, *Water Resour. Res.*, *27*(9), 2171–2179, doi:10.1029/91WR01243.
- Cuffey, K. M., and G. D. Clow (1997), Temperature, accumulation, and ice sheet elevation in central Greenland through the last deglacial transition, *J. Geophys. Res.*, *102*, 26,383–26,396, doi:10.1029/96JC03981.
- Doyle, S. H., *et al.* (2015), Amplified melt and flow of the Greenland ice sheet driven by late-summer cyclonic rainfall, *Nat. Geosci.*, *8*(8), 647–653, doi:10.1038/ngeo2482.
- Faber, A.-K., B. Vinther, J. Sjolte, and R. Anker Pedersen (2015), How does sea ice influence the isotopic composition of Arctic precipitation?, in *EGU General Assembly Conference Abstracts*, vol. 17, pp. 5562, Geophys. Res. Abstr., Vienna, Austria.
- Gao, L., Y.-J. Tsai, and Y. Huang (2012), Assessing the rate and timing of leaf wax regeneration in *Fraxinus americana* using stable hydrogen isotope labeling, *Rapid Commun. Mass Spectrom.*, *26*(19), 2241–2250, doi:10.1002/rcm.6348.
- IAEA/WMO (2011), Global network of isotopes in precipitation, The GNIP Database.
- Jonsson, C. E., M. J. Leng, G. C. Rosqvist, J. Seibert, and C. Arrowsmith (2009), Stable oxygen and hydrogen isotopes in sub-Arctic lake waters from northern Sweden, *J. Hydrol.*, *376*(1–2), 143–151, doi:10.1016/j.jhydrol.2009.07.021.
- Jouzel, J., *et al.* (1997), Validity of the temperature reconstruction from water isotopes in ice cores, *J. Geophys. Res.*, *102*, 26,471–26,487, doi:10.1029/97JC01283.
- Kobashi, T., K. Kawamura, J. P. Severinghaus, J.-M. Barnola, T. Nakaegawa, B. M. Vinther, S. J. Johnsen, and J. E. Box (2011), High variability of Greenland surface temperature over the past 4000 years estimated from trapped air in an ice core, *Geophys. Res. Lett.*, *38*, L21501, doi:10.1029/2011GL049444.
- Kopec, B. G., X. Feng, F. A. Michel, and E. S. Posmentier (2016), Influence of sea ice on Arctic precipitation, *Proc. Natl. Acad. Sci. U.S.A.*, *113*(1), 46–51, doi:10.1073/pnas.1504633113.
- Krawczyk, D. W., A. Witkowski, J. Lloyd, M. Moros, J. Harff, and A. Kuijpers (2013), Late-Holocene diatom derived seasonal variability in hydrological conditions off Disko Bay, West Greenland, *Quat. Sci. Rev.*, *67*, 93–104, doi:10.1016/j.quascirev.2013.01.025.
- Laskar, J., P. Robutel, F. Joutel, M. Gastineau, A. C. M. Correia, and B. Levrard (2004), A long-term numerical solution for the insolation quantities of the Earth, *Astron. Astrophys.*, *428*(1), 261–285, doi:10.1051/0004-6361:20041335.

- Lecavalier, B. S., et al. (2014), A model of Greenland ice sheet deglaciation constrained by observations of relative sea level and ice extent, *Quat. Sci. Rev.*, *102*, 54–84, doi:10.1016/j.quascirev.2014.07.018.
- Ledu, D., A. Rochon, A. de Vernal, F. Barletta, and G. St-Onge (2010), Holocene sea ice history and climate variability along the main axis of the Northwest Passage, Canadian Arctic, *Paleoceanography*, *25*, PA2213, doi:10.1029/2009PA001817.
- Markus, T., J. C. Stroeve, and J. Miller (2009), Recent changes in Arctic sea ice melt onset, freezeup, and melt season length, *J. Geophys. Res.*, *114*, C12024, doi:10.1029/2009JC005436.
- NCDC NOAA (2012), Global historical climatology network.
- Nichols, J. E., M. Walcott, R. Bradley, J. Pilcher, and Y. Huang (2009), Quantitative assessment of precipitation seasonality and summer surface wetness using ombrotrophic sediments from an Arctic Norwegian peatland, *Quat. Res.*, *72*(3), 443–451, doi:10.1016/j.yqres.2009.07.007.
- Ohmura, A., and N. Reeh (1991), New precipitation and accumulation maps for Greenland, *J. Glaciol.*, *37*, 140–148.
- ORNL DAAC (2008), MODIS collection 5 land products global subsetting and visualization tool, ORNL DAAC, Oak Ridge, Tenn.
- Quellet-Bernier, M.-M., A. de Vernal, C. Hillaire-Marcel, and M. Moros (2014), Paleoceanographic changes in the Disko Bugt area, West Greenland, during the Holocene, *Holocene*, *24*(11), 1573–1583, doi:10.1177/0959683614544060.
- Perner, K., M. Moros, A. Jennings, J. M. Lloyd, and K. L. Knudsen (2013), Holocene palaeoceanographic evolution off West Greenland, *Holocene*, *23*(3), 374–387, doi:10.1177/0959683612460785.
- Rasmussen, S. O., et al. (2013), A first chronology for the North Greenland Eemian Ice Drilling (NEEM) ice core, *Clim. Past*, *9*(6), 2713–2730, doi:10.5194/cp-9-2713-2013.
- Sachse, D., et al. (2012), Molecular paleohydrology: Interpreting the hydrogen-isotopic composition of lipid biomarkers from photosynthesizing organisms, *Annu. Rev. Earth Planet. Sci.*, *40*(1), 221–249, doi:10.1146/annurev-earth-042711-105535.
- Shanahan, T. M., K. A. Hughen, L. Ampel, P. E. Sauer, and K. Fornace (2013), Environmental controls on the $^{2}\text{H}/^{1}\text{H}$ values of terrestrial leaf waxes in the eastern Canadian Arctic, *Geochim. Cosmochim. Acta*, *119*, 286–301, doi:10.1016/j.gca.2013.05.032.
- Sodemann, H., C. Schwierz, and H. Wernli (2008), Interannual variability of Greenland winter precipitation sources: Lagrangian moisture diagnostic and North Atlantic Oscillation influence, *J. Geophys. Res.*, *113*, D03107, doi:10.1029/2007JD008503.
- Thomas, E. K., J. P. Briner, Y. Axford, D. R. Francis, G. H. Miller, and I. R. Walker (2011), A 2000-yr-long multi-proxy lacustrine record from eastern Baffin Island, Arctic Canada reveals first millennium AD cold period, *Quat. Res.*, *75*(3), 491–500, doi:10.1016/j.yqres.2011.03.003.
- Thomas, E. K., S. McGrane, J. Briner, and Y. Huang (2012), Leaf wax $\delta^2\text{H}$ and varve-thickness climate proxies from proglacial lake sediments, Baffin Island, Arctic Canada, *J. Paleolimnol.*, *48*(1), 193–207, doi:10.1007/s10933-012-9584-7.
- Tipple, B. J., M. A. Berke, C. E. Doman, S. Khachatryan, and J. R. Ehleringer (2013), Leaf-wax *n*-alkanes record the plant-water environment at leaf flush, *Proc. Natl. Acad. Sci. U.S.A.*, *110*(7), 2659–2664, doi:10.1073/pnas.1213875110.
- de Vernal, A., C. Hillaire-Marcel, A. Rochon, B. Fréchet, M. Henry, S. Solignac, and S. Bonnet (2013), Dinocyst-based reconstructions of sea ice cover concentration during the Holocene in the Arctic Ocean, the northern North Atlantic Ocean and its adjacent seas, *Quat. Sci. Rev.*, *79*, 111–121, doi:10.1016/j.quascirev.2013.07.006.
- Young, N. E., and J. P. Briner (2015), Holocene evolution of the western Greenland Ice Sheet: Assessing geophysical ice-sheet models with geological reconstructions of ice-margin change, *Quat. Sci. Rev.*, *114*, 1–17, doi:10.1016/j.quascirev.2015.01.018.
- Young, N. E., J. P. Briner, D. H. Rood, R. C. Finkel, L. B. Corbett, and P. R. Bierman (2013), Age of the Fjord Stade moraines in the Disko Bugt region, western Greenland, and the 9.3 and 8.2 ka cooling events, *Quat. Sci. Rev.*, *60*, 76–90, doi:10.1016/j.quascirev.2012.09.028.